Engineering Applications of Artificial Intelligence 121 (2023) 106027

Contents lists available at ScienceDirect

Engineering Applications of Artificial Intelligence

journal homepage: www.elsevier.com/locate/engappai

A fractal belief KL divergence for decision fusion

Jie Zeng, Fuyuan Xiao *

School of Big Data and Software Engineering, Chongqing University, No. 55 South University Town Road, Shapingba District, Chongqing 401331, China

ARTICLE INFO

Keywords:
Dempster–Shafer evidence theory
Fractal belief KL divergence
Conflict management
Multi-source data fusion
Classification

ABSTRACT

Dempster–Shafer (D–S) evidence theory is useful in the realm of multi-source data fusion. However, a counterintuitive result may be obtained when the belief probability assignments (BPAs) are highly conflicting. To overcome this flaw, in this paper a symmetric fractal-based belief Kullback–Leibler divergence (FBD_{SKL}) is proposed. It is used to measure the divergence between BPAs, and is more capable than the existing belief divergence methods in measuring the conflict between two BPAs in numerical examples. Furthermore, the proposed FBD_{SKL} is proved to have desirable properties including nonnegativity, nondegeneracy and symmetry. To apply FBD_{SKL} divergence measure to practical problems, a novel FBD_{SKL}-based multi-source data fusion (FBD_{SKL}-MSDF) algorithm is designed. Through comparisons with the well-known related methods, the proposed FBD_{SKL}-MSDF algorithm is validated to be superior and more robust. Finally, the proposed FBD_{SKL}-MSDF is applied to two real-world classification problems to verify its high practicability.

1. Introduction

Multi-source data fusion is a technique for combining information and generating an eventual decision target in real-world applications (Li et al., 2021). One of the most challenging issues is how to handle the highly conflicting multi-source data. To be specific, due to the ambiguity, inconsistency or even incorrectness of the multi-source data, it is of great importance that the degree of confidence of data given by every source should be quantified (Yager, 2021), so the inappropriate data are confidence-weaken or close to be ignored. In the field of multi-source data fusion, there have been many renowned theories to model and handle different types of uncertainties, including fuzzy set (Tao et al., 2021), D numbers (Lai and Liao, 2021) and probability distribution (Wu et al., 2022). Furthermore, these theories have been widely applied in various realms, such as representation learning (Fujita and Ko, 2020), medical diagnosis (Lai and Cheong, 2020; Cao et al., 2019), fault diagnosis (Meng et al., 2022), dynamics analysis (Wang et al., 2022b,a), velocity measurement (Wei et al., 2021), graph clustering (Chu et al., 2022), classification (Miao et al., 2023), group decision making (Fu et al., 2022; Zhou et al., 2022; Mao et al., 2020), and others (Wang et al., 2023).

One of the fundamental theory basis of multi-source data fusion is Dempster–Shafer (D–S) evidence theory (Dempster, 1967; Shafer, 1976). The main advantages of D–S evidence theory are that it can quantify the belief value of both single targets and unions of objects. In addition, D–S evidence theory conducts uncertainty reasoning through the Dempster combination rule in a flexible and effective way without the need for prior information. Because of the effectiveness and flexibility in modeling uncertainty, D–S evidence theory has widespread applications in various realms of information fusion, such as EEG data analysis (Zhu et al., 2022), decision making (Liu et al., 2020b), rescuer assignments (Fei and Wang, 2022a), social network analysis (Ni et al., 2021) and risk evaluation (Liu et al., 2022; Chen and Deng, 2022), output control (Chang et al., 2022), prediction of emergency (Fei and Wang, 2022b), pattern classification (Xiao et al., 2022a; Liu et al., 2020a; Xu et al., 2020), cardiac interbeat interval time series analysis (Cui et al., 2022) and database retrieval (Yager et al., 2019).

However, the open issue in Dempster's method is that it cannot handle highly conflicting BPAs and may generate counterintuitive results. To address this problem, there are many related methods proposed to measure the uncertainty and handle those conflicting BPAs. To be specific, one of the existing related works for this purpose is Murphy's approach (Murphy, 2000), which implements a numeric-average preprocessing to the BPAs. Then, Deng et al. (2004) propose a distance matrix to estimate the supporting degrees between given BPAs. Except for these methods, Shang et al. (2022) put forward an autoencoder-K-Means approach to calculate the compound credibility for conflicting BPAs; Xiong et al. (2021) take another view by modeling networks to combine the conflict evidence. Furthermore, some researchers address this issue from another perspective of belief divergence (Xiao et al., 2022b; Xiao, 2022a). For example, Xiao (2019) proposes a belief Jensen–Shannon (BJS) measure based on the Jensen–Shannon (JS) divergence.

In these many uncertainty measurement methods, belief divergence indicates a novel and promising orientation in information fusion.

* Corresponding author.
E-mail address: xiaofuyuan@cqu.edu.cn (F. Xiao).

https://doi.org/10.1016/j.engappai.2023.106027
Received 18 August 2022; Received in revised form 2 January 2023; Accepted 18 February 2023
Available online 1 March 2023
0952-1976/© 2023 Elsevier Ltd. All rights reserved.

Therefore, in this paper, the main focus is to conduct research on belief divergence to address multi-source fusion problems. By conducting thorough research on the existing belief divergence methods, it is found that in some cases, these belief divergence methods may yield counterintuitive results, and details will be discussed in Section 2.2.2. Furthermore, these counterintuitive divergence values may exert an influence on the results of algorithm applications such as pattern recognition and classification. Thus, how to construct a belief divergence model is still an open issue. In this paper, to address this issue, a novel belief divergence measurement method is proposed to handle these problems to benefit information fusion.

It is well known that self-similarity is a prominent property of fractal theory. To be specific, the integral objects on the macro level, however, are made of similar parts. There are some fractal-based methods in the uncertainty measurement, such as probability transformation (Chen et al., 2021), information volume (Deng, 2020a; Zhou and Deng, 2022) and information dimension (Qiang et al., 2022). Fractal methods can measure the overlapping degree between events in the processing of uncertain information (Deng and Cui, 2021). It is noticed that the subsets in different BPAs may be partially supported. Therefore, in the proposed divergence measurement, a fractal process is implemented to transform the BPAs into their fractal forms. The fractal-transformed BPAs show the intrinsic similarities between the original BPAs more intuitively. Inspired by information volume and its extensions (Deng, 2020a; Zhou and Deng, 2022), a novel symmetric fractal-based belief KL divergence, also called FBD_{SKL}, is proposed to appropriately measure the conflict between BPAs. The following is a list of the study's main contributions:

- The newly defined FBD_{SKL} method has certain benefits owing to its four proved desirable properties, and it provides a more convincing measure solution to quantify the conflict degrees between mutual evidence functions.
- Based on the newly defined FBD_{SKL}, a novel FBD_{SKL}-based multi-source data fusion (FBD_{SKL}-MSDF) algorithm is proposed.
- FBD_{SKL}-MSDF is conducted with a numeric experiment and applied in two classification problems and reveals high recognition accuracy and strong robustness.

The remaining contexts are organized as follows. Section 2 summarizes the preliminaries of evidence theory and existing related methods in the realm. In Section 3, a fractal-based belief Kullback–Leibler divergence measure is proposed. In Section 4, based on the FBD_{SKL}, a novel algorithm for multi-source data fusion (FBD_{SKL}-MSDF) is proposed. In Section 5, experiments of multi-source data fusion on target recognition and a sensitivity analysis are conducted to verify the superiority and robustness of FBD_{SKL}-MSDF. In Section 6, application comparisons with the well-known existing methods are respectively implemented. Finally, in Section 7, conclusions of this research are drawn.

2. Preliminaries

2.1. Dempster–Shafer evidence theory

D–S evidence theory, as a generalization of Bayes probability theory, is a great tool for dealing with ambiguous data (Dempster, 1967; Shafer, 1976), so that it has been extended to theories including random permutation set (Deng, 2022; Deng and Deng, 2022), evidence reasoning (Tang et al., 2021; Huang et al., 2023; Zhang and Xiao, 2022), generalized quantum evidence theory (Xiao, 2022b; Xiao and Pedrycz, 2022), etc.

Definition 2.1 (*Frame of Discernment*)**.** Let Θ be a set of events which are mutually exclusive and collectively exhaustive. Thus we have

$$\Theta = \{H_1, H_2, \ldots, H_k, \ldots, H_n\}, \tag{1}$$

which is defined as a frame of discernment.

Comprised with all the subsets in Θ, The power set of Θ, denoted as 2^Θ, is defined as

$$2^\Theta = \{\varnothing, \{H_1\}, \{H_2\}, \ldots, \{H_n\}, \{H_1, H_2\}, \ldots, \{H_1, H_2, \ldots, H_k\}, \ldots, \Theta\}, \tag{2}$$

where $\varnothing$ stands for an empty set. It is obvious that the number of subsets in 2^Θ is 2^n (Song and Deng, 2021).

If $A \in 2^\Theta$, then A is called a hypothesis.

Definition 2.2 (*Mass Function*)**.** In the frame of discernment Θ, a mass function from 2^Θ, denoted by m, is defined as:

$$m : 2^\Theta \to [0, 1], \tag{3}$$

which also satisfies the following conditions:

$$\sum_{A \in 2^\Theta} m(A) = 1 \ and \ m(\varnothing) = 0, \tag{4}$$

where $m(A)$ quantifies the belief value of hypothesis A. In D–S theory, a mass function m is also named a BPA. If $m(A) > 0$, A is called a focal element. Because BPA is effective to express uncertainty, it has been well studied (Li et al., 2022; Deng, 2020b; Zhou et al., 2023).

Definition 2.3 (*Dempster's Rule of Combination*)**.** Let m_1 and m_2 be two independent BPAs in the frame of discernment Θ. So the combined BPA $m = m_1 \oplus m_2$ is defined as:

$$m(A) = \begin{cases} \frac{1}{1-K} \sum_{B \cap C = A} m_1(B) m_2(C), & A \neq \varnothing, \\ 0, & A = \varnothing, \end{cases} \tag{5}$$

where

$$K = \sum_{B \cap C = \varnothing} m_1(B) m_2(C), \tag{6}$$

and $B, C \in 2^\Theta$. Universally, we call K as the coefficient to measure the conflicts between m_1 and m_2.

Note that from Eqs. (5) and (6), the range of K is inferred: $0 \leq K < 1$.

2.2. Belief divergence methods

2.2.1. BJS divergence and $\mathfrak{B}$ divergence measure for two BPAs

A Belief Jensen–Shannon divergence (BJS divergence) was presented by Xiao (2019) to quantify the conflict between BPAs.

Definition 2.4 (*BJS Divergence Measure*)**.** Let m_1 and m_2 be two independent BPAs, and A is a hypothesis in the frame of discernment Θ. A BJS divergence measure between two BPAs m_1 and m_2 is defined as follows:

$$BJS(m_1, m_2) = \frac{1}{2}[S\left(m_1, \frac{(m_1 + m_2)}{2}\right) + S\left(m_2, \frac{(m_1 + m_2)}{2}\right)], \tag{7}$$

where $S\left(m_1, m_2\right) = \sum_{i=1}^{2^n-1} m_1\left(A_i\right) \log \frac{m_1(A_i)}{m_2(A_i)}$ and $\sum_{i=1}^{2^n-1} m_j(A_i) = 1$ (j = 1, 2).

So $BJS(m_1, m_2)$ divergence is also expanded, and expressed with the following formula:

$$\begin{aligned} BJS(m_1, m_2) = & \frac{1}{2} \sum_{i=1}^{2^n-1} m_1(A_i) \log\left(\frac{2m_1(A_i)}{m_1(A_i) + m_2(A_i)}\right) \\ & + \frac{1}{2} \sum_{i=1}^{2^n-1} m_2(A_i) \log\left(\frac{2m_2(A_i)}{m_1(A_i) + m_2(A_i)}\right). \end{aligned} \tag{8}$$

Definition 2.5 ($\mathfrak{B}$ *Divergence Measure for Two BPAs*)**.** Let m_1 and m_2 be two BPAs in the frame of discernment Θ, in which there are n mutually exclusive hypotheses. In this frame of discernment Θ, let A_i and A_j be

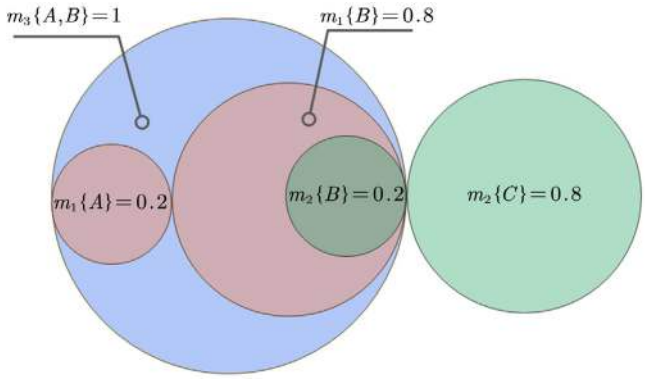

Fig. 1. The overlap-relationship between focal elements of BPAs.

two hypotheses from m_1 and m_2 ($1 \leqslant i, j \leqslant 2^n - 1$). The $\mathfrak{B}$ belief divergence measure between m_1 and m_2 is defined as

$$\begin{aligned}\mathfrak{B}(m_1, m_2) =& \frac{1}{2}\sum_{i=1}^{2^n-1}\sum_{j=1}^{2^n-1} m_1(A_i)\log\frac{m_1(A_i)}{\frac{1}{2}m_1(A_i)+\frac{1}{2}m_2(A_j)}\frac{|A_i\cap A_j|}{|A_j|}\\ &+\frac{1}{2}\sum_{i=1}^{2^n-1}\sum_{j=1}^{2^n-1} m_2(A_j)\log\frac{m_2(A_j)}{\frac{1}{2}m_1(A_i)+\frac{1}{2}m_2(A_j)}\frac{|A_i\cap A_j|}{|A_i|},\end{aligned} \tag{9}$$

where the $|A_i|$ represents the cardinality of subset of A_i, and $|A_i \cap A_j|$ equals the cardinality of intersection subset between A_i and A_j.

Obviously, when the focal elements are only constituted with singletons, that is: $\frac{|A_i\cap A_j|}{|A_i|} = 0$ or $\frac{|A_i\cap A_j|}{|A_i|} = 1$ ($1 \leqslant i, j \leqslant 2^n - 1$), the $\mathfrak{B}$ divergence will degenerate into BJS divergence:

$$\begin{aligned}\mathfrak{B}(m_1, m_2) =& \frac{1}{2}\sum_{i=1}^{2^n-1} m_1(A_i)\log\frac{m_1(A_i)}{\frac{1}{2}m_1(A_i)+\frac{1}{2}m_2(A_i)}\\ &+\frac{1}{2}\sum_{i=1}^{2^n-1} m_2(A_i)\log\frac{m_2(A_i)}{\frac{1}{2}m_1(A_i)+\frac{1}{2}m_2(A_i)}.\end{aligned} \tag{10}$$

2.2.2. Analysis of BJS and $\mathfrak{B}$ divergence measure methods

In this subsection, numeric examples of BJS divergence measure and $\mathfrak{B}$ divergence measure applied in evidence theory are presented. Furthermore, based on these concrete numeric examples, the performance of these divergence measures is analyzed and becomes the motivation of our proposed divergence method.

BJS divergence, a generalized model based on Jensen–Shannon divergence measure, is presented to measure the difference between BPAs. However, the limitation of BJS divergence is obvious, which neglects the correlation between subsets of BPAs. Here follows a concrete example to elaborate this limitation.

Example 1. Suppose that there are three independent BPAs: m_1, m_2 and m_3 in the frame of discernment $\Theta = \{A, B, C\}$:

$$\begin{aligned} m_1 &: \quad m_1(\{A\}) = 0.2, \quad m_1(\{B\}) = 0.8;\\ m_2 &: \quad m_2(\{B\}) = 0.2, \quad m_2(\{C\}) = 0.8;\\ m_3 &: \quad m_3(\{A, B\}) = 1.\end{aligned}$$

According to the three BPAs above, it is noticed that m_1 assigns its belief value to two singletons $\{A\}$ and $\{B\}$, and m_2 also assigns its belief value to two singletons $\{B\}$ and $\{C\}$, while m_3 completely supports the subset $\{A, B\}$. As shown in Fig. 1, the focal-element-relationship of three BPAs presented by overlapped circles is in line with intuition: the pair of m_1 and m_3 is more mutually supportive than the pair of m_2 and m_3. In other words, the former pair of m_1 and m_3, which is less conflicting, should have lower divergence than the latter pair of m_2 and m_3:

$$div_{\text{ex}}\left(m_1, m_3\right) < div_{\text{ex}}\left(m_2, m_3\right),$$

where the function of $div_{\text{ex}}\left(m_i, m_j\right)$ denotes a relatively appropriate measure between m_i and m_j.

However, the outcome yielded by the BJS divergence measure is as follows:

$$BJS(m_1, m_3) = BJS(m_2, m_3) = 1.$$

This result is not coordinated with intuition and reveals that the BJS divergence does not take these similarities between subsets into consideration. To overcome the limitation of BJS divergence measure, the later presented $\mathfrak{B}$ divergence measure seems a promotion of BJS divergence measure, because it takes the overlap-relationship of different BPAs into account.

The $\mathfrak{B}$ divergence measure seems a promotion of BJS divergence measure, as it takes into account the similarities between subsets of different BPAs. As is pointed out in Example 1, an expected divergence measure yields the consequence: $div_{\text{ex}}\left(m_1, m_3\right) < div_{\text{ex}}\left(m_2, m_3\right)$ in that case. The $\mathfrak{B}$ divergence measure is implemented in Example 1 and outputs the results:

$$\begin{aligned}&\mathfrak{B}(m_1, m_3) = 1.3313;\\ &\mathfrak{B}(m_2, m_3) = 3.3152.\end{aligned}$$

So we have:

$$\mathfrak{B}(m_1, m_3) < \mathfrak{B}(m_2, m_3).$$

This result is in line with the expected answer in Example 1. However, $\mathfrak{B}$ divergence measure also has a limitation, which is discussed in Example 2.

Example 2. Suppose that there are two BPAs m_1 and m_2 in the frame of discernment $\Theta = \{A, B\}$, where variable α is in the interval of $[0, 1]$:

$$\begin{aligned} m_1 &: m_1(\{A\}) = \alpha,\ m_1(\{A, B\}) = 1 - \alpha;\\ m_2 &: m_2(\{A\}) = 1.\end{aligned}$$

With α ranging from 0 to 1, the value of $m_1(A)$ simultaneously varies from 0 to 1, while $m_1(A, B)$ decreases from 1 to 0 on the other hand. It is intuitively obvious that the difference between m_1 and m_2 is lowing. Finally, when $\alpha = 1$, m_1 is completely equivalent to m_2. But, as shown in Fig. 2, in the process of increment of α from 0 to 1, an intuition-opposite turning point is revealed in the curve of $\mathfrak{B}\left(m_1, m_2\right)$. However, the conflict should have been reduced when m_1 and m_2 tend to be increasingly mutually supportive. So on account of this limitation in $\mathfrak{B}$ divergence, a new divergence measure needs to be explored to more appropriately quantify the divergence between BPAs.

3. A fractal-based belief KL divergence measure

In this section, combined with a fractal preprocess, a new belief Kullback–Leibler (KL) divergence is devised. In order to obtain better properties of this model, a symmetric fractal-based belief KL divergence measure is proposed. Additionally, numerical examples are given to illustrate how the proposed divergence measure can overcome the limitations of BJS and $\mathfrak{B}$ divergences. Then, properties are analyzed and proved, which can benefit practical problems.

3.1. The process of probability transformation based on fractal

BPA can express more information by assigning the mass functions to the multi-element focal elements. Thus, how to reasonably transform BPA into its fractal form is the key to obtaining essential information about the BPA. Inspired by pignistic probability transformation (Zhou and Deng, 2022), a fractal splitting of a BPA is defined as follows:

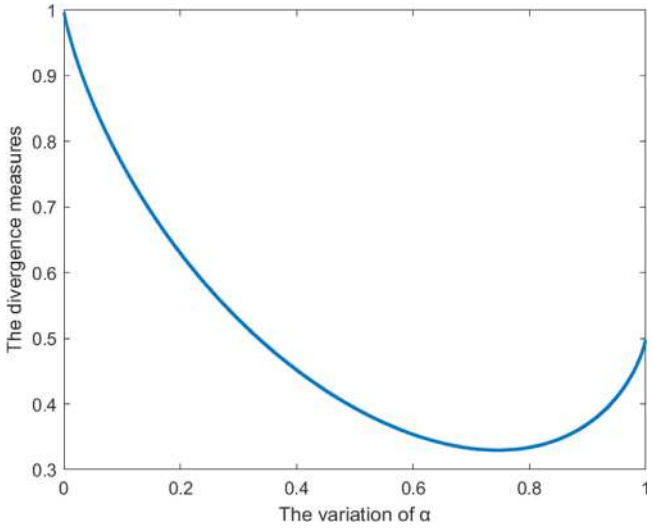

Fig. 2. The $\mathfrak{B}$ divergence measure.

Definition 3.1 (*A Fractal Splitting of One BPA*)**.** Let m_k be one BPA in the frame of discernment Θ, where $k = 1, 2, \ldots$. The transformation from basic probability assignment (BPA) m_k into fractal-based basic probability assignment (FBBPA) m_{F_k} process is defined as (Zhou and Deng, 2022):

$$m_{F_k}(H_i) = \sum_{H_i \subseteq G_i} \frac{m_k(G_i)}{2^{|G_i|} - 1}, \tag{11}$$

This process can be shown in Fig. 3. It is noticed that for every multiset in the given BPA, it is uniformly split into its power set. As is discussed in Zhou and Deng (2022), the FBBPA is neither BPA nor probability distribution, but it describes the characteristics of BPA from the perspective of probability. Therefore, inspired by this splitting process, the divergence measurement can be conducted with fractal process. Furthermore, this proposed FBD_{KL} in Section 3.2 and FBD_{SKL} in Section 3.3 are the first belief divergence models which are incorporated with the fractal concept to measure the dissimilarity between two BPAs.

3.2. Fractal-based belief KL divergence

In this section, inspired by Deng entropy and fractal concept, a fractal-based belief KL divergence is proposed to measure conflict between BPAs.

Definition 3.2 (*Fractal-based Belief KL Divergence Measure*)**.** Let m_1 and m_2 be two BPAs in the frame of discernment Θ. The belief divergence FBD_{KL} between m_1 and m_2 is defined as:

$$FBD_{KL}(m_1, m_2) = \sum_{i=1}^{2^n-1} m_{F_1}(H_i) \log \frac{m_{F_1}(H_i)}{m_{F_2}(H_i)}, \tag{12}$$

where $m_{F_k}(H_i)$ is based on fractal process and is defined as:

$$m_{F_k}(H_i) = \sum_{H_i \subseteq G_i} \frac{m_k(G_i)}{2^{|G_i|} - 1},$$

where $k = 1, 2$ and $H_i, G_i \subseteq \Theta$.

Properties. Let m_1, m_2 and m_3 be three random BPAs, and H_i is a focal element in the frame of discernment Θ ($1 \leqslant i \leqslant 2^n - 1$). And the cardinality of H_i, denoted as $|H_i|$, represents the number of elements in H_i. Then, three properties of FBD_{KL} are defined as follows.

(1) Asymmetry: $FBD_{KL}(m_1, m_2) \neq FBD_{KL}(m_2, m_1)$.
(2) Unboundedness: $-\infty < FBD_{KL}(m_1, m_2) < +\infty$.
(3) $FBD_{KL}(m_1, m_2) = D_{KL}(m_1, m_2)$, when $\forall |H_i| = 1$.

3.3. Symmetric fractal-based belief KL divergence

In this section, the FBD_{KL} function is reinforced by constructing it into a symmetric structure FBD_{SKL}, which obtains better properties applied to practical problems. So, a symmetric fractal-based belief KL divergence is elaborated as follows.

Definition 3.3 (*Symmetric Fractal-based Belief KL Divergence Measure*)**.** Let m_1 and m_2 be two belief functions in the frame of discernment Θ. The symmetric fractal-based belief KL divergence $FBD_{SKL}(m_1, m_2)$ is defined as:

$$FBD_{SKL}(m_1, m_2) = \frac{1}{2} \sum_{i=1}^{2^n-1} \begin{bmatrix} m_{F_1}(H_i) \log \frac{m_{F_1}(H_i)}{\sqrt{m_{F_1}(H_i) \times m_{F_2}(H_i)}} \\ + m_{F_2}(H_i) \log \frac{m_{F_2}(H_i)}{\sqrt{m_{F_2}(H_i) \times m_{F_1}(H_i)}} \end{bmatrix}, \tag{13}$$

where $m_{F_k}(H_i)$ is based on fractal process and is defined as:

$$m_{F_k}(H_i) = \sum_{H_i \subseteq G_i} \frac{m_k(G_i)}{2^{|G_i|} - 1},$$

where $k = 1, 2$ and $H_i, G_i \subseteq \Theta$.

Theorem 1. *The symmetric fractal-based belief KL divergence has properties (1)–(4) below for measurement.*

Properties. Let m_1, m_2 and m_3 be three random BPAs, and H_i is a focal element in the frame of discernment Θ ($1 \leqslant i \leqslant 2^n - 1$). The cardinality of H_i, denoted as $|H_i|$, represents the number of exclusive elements in H_i. Then, four properties are defined as follows.

(1) Nonnegativity: $0 \leqslant FBD_{SKL}(m_1, m_2) < +\infty$.
(2) Nondegeneracy: $FBD_{SKL}(m_1, m_2) = 0$ if and only if $m_1 = m_2$.
(3) Symmetry: $FBD_{SKL}(m_1, m_2) = FBD_{SKL}(m_2, m_1)$.
(4) $FBD_{SKL}(m_1, m_2) = \frac{1}{4}(D_{KL}(m_1, m_2) + D_{KL}(m_2, m_1))$, when $\forall |H_i| = 1$.

Proof. (1) $FBD_{SKL}(m_1, m_2)$ could be deformed as follows:

$$\begin{aligned}
FBD_{SKL}(m_1, m_2) &= \frac{1}{2} \sum_{i=1}^{2^n-1} \begin{bmatrix} m_{F_1}(H_i) \log \frac{m_{F_1}(H_i)}{\sqrt{m_{F_1}(H_i) \times m_{F_2}(H_i)}} \\ + m_{F_2}(H_i) \log \frac{m_{F_2}(H_i)}{\sqrt{m_{F_2}(H_i) \times m_{F_1}(H_i)}} \end{bmatrix} \\
&= \frac{1}{2} \sum_{i=1}^{2^n-1} \begin{bmatrix} m_{F_1}(H_i) \log \sqrt{\frac{m_{F_1}(H_i)}{m_{F_2}(H_i)}} \\ + m_{F_2}(H_i) \log \sqrt{\frac{m_{F_2}(H_i)}{m_{F_1}(H_i)}} \end{bmatrix} \\
&= \frac{1}{2} \sum_{i=1}^{2^n-1} \begin{bmatrix} \frac{1}{2} m_{F_1}(H_i) \log \frac{m_{F_1}(H_i)}{m_{F_2}(H_i)} \\ + \frac{1}{2} m_{F_2}(H_i) \log \frac{m_{F_2}(H_i)}{m_{F_1}(H_i)} \end{bmatrix} \\
&= \frac{1}{4} \sum_{i=1}^{2^n-1} \begin{bmatrix} m_{F_1}(H_i) (\log m_{F_1}(H_i) - \log m_{F_2}(H_i)) \\ + m_{F_2}(H_i) (\log m_{F_2}(H_i) - \log m_{F_1}(H_i)) \end{bmatrix} \\
&= \frac{1}{4} \sum_{i=1}^{2^n-1} \begin{bmatrix} m_{F_1}(H_i) \log m_{F_1}(H_i) - m_{F_1}(H_i) \log m_{F_2}(H_i) \\ + m_{F_2}(H_i) \log m_{F_2}(H_i) - m_{F_2}(H_i) \log m_{F_1}(H_i) \end{bmatrix} \\
&= \frac{1}{4} \sum_{i=1}^{2^n-1} \begin{bmatrix} \log m_{F_1}(H_i) (m_{F_1}(H_i) - m_{F_2}(H_i)) \\ - \log m_{F_2}(H_i) (m_{F_1}(H_i) - m_{F_2}(H_i)) \end{bmatrix} \\
&= \frac{1}{4} \sum_{i=1}^{2^n-1} \left[(\log m_{F_1}(H_i) - \log m_{F_2}(H_i)) (m_{F_1}(H_i) - m_{F_2}(H_i)) \right].
\end{aligned}$$

It is obvious that:

$$\left(\log m_{F_1}(H_i) - \log m_{F_2}(H_i) \right) \left(m_{F_1}(H_i) - m_{F_2}(H_i) \right) \geqslant 0.$$

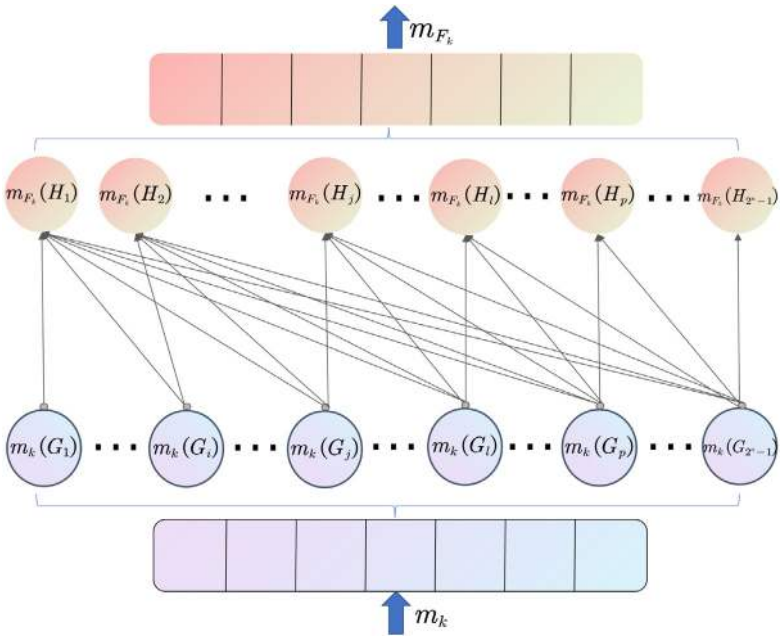

Fig. 3. The fractal process of BPA m_k into FBBPA m_{F_k}.

So, for $i = 1, \ldots, 2^n - 1$, any subitem in $FBD_{SKL}(m_1, m_2)$

$$\frac{1}{2}\left[m_{F_1}(H_i)\log\frac{m_{F_1}(H_i)}{\sqrt{m_{F_1}(H_i)\times m_{F_2}(H_i)}} + m_{F_2}(H_i)\log\frac{m_{F_2}(H_i)}{\sqrt{m_{F_2}(H_i)\times m_{F_1}(H_i)}}\right]$$

satisfies that:

$$\frac{1}{2}\left[m_{F_1}(H_i)\log\frac{m_{F_1}(H_i)}{\sqrt{m_{F_1}(H_i)\times m_{F_2}(H_i)}} + m_{F_2}(H_i)\log\frac{m_{F_2}(H_i)}{\sqrt{m_{F_2}(H_i)\times m_{F_1}(H_i)}}\right] \geqslant 0$$

Therefore, it is concluded that:

$$FBD_{SKL}(m_1, m_2) \geqslant 0.$$

On the other hand, for $1 \leqslant i \leqslant 2^n - 1$, it is already proved that any subitem in $FBD_{SKL}(m_1, m_2)$ satisfies:

$$\frac{1}{2}\left[m_{F_1}(H_i)\log\frac{m_{F_1}(H_i)}{\sqrt{m_{F_1}(H_i)\times m_{F_2}(H_i)}} + m_{F_2}(H_i)\log\frac{m_{F_2}(H_i)}{\sqrt{m_{F_2}(H_i)\times m_{F_1}(H_i)}}\right] \geqslant 0.$$

In addition, the figure of this two-dimensional function:

$$\frac{1}{4}\left(\log m_{F_1}(H_i) - \log m_{F_2}(H_i)\right)\left(m_{F_1}(H_i) - m_{F_2}(H_i)\right)$$

is shown in Fig. 4.

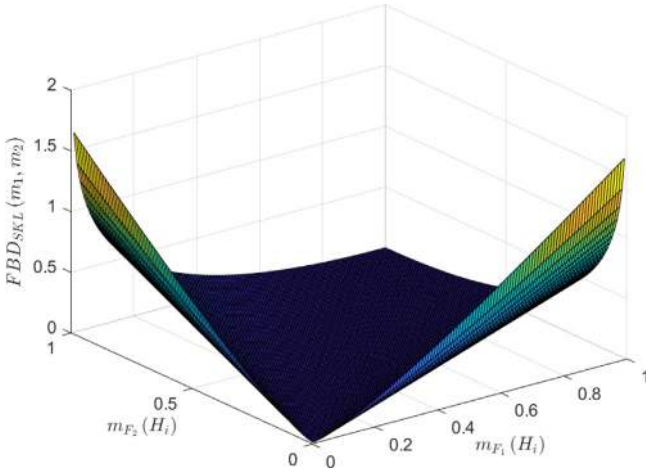

Fig. 4. The value variation of subitem function in $FBD_{SKL}(m_1, m_2)$.

According to the nonnegativity of any subitem in $FBD_{SKL}(m_1, m_2)$, when $i = p$, it is considered that this specific subitem satisfies:

$$\frac{1}{4}\left(\log m_{F_1}(H_p) - \log m_{F_2}(H_p)\right)\left(m_{F_1}(H_p) - m_{F_2}(H_p)\right) \leqslant FBD_{SKL}(m_1, m_2)$$

Thus, when $\left(\log m_{F_1}(H_p) - \log m_{F_2}(H_p)\right)$ converges the value of positive infinity, that is:

$$\left(\log m_{F_1}(H_p) - \log m_{F_2}(H_p)\right) \to +\infty,$$

it is obvious that this subitem satisfies:

$$\frac{1}{4}\left(\log m_{F_1}(H_p) - \log m_{F_2}(H_p)\right)\left(m_{F_1}(H_p) - m_{F_2}(H_p)\right) \to +\infty.$$

So, it is summarized that in this case:

$$FBD_{SKL}(m_1, m_2) \to +\infty.$$

Therefore, a conclusion is drawn that the upper bound of $FBD_{SKL}(m_1, m_2)$ does not exist.

Hence, the nonnegativity of FBD_{SKL} divergence measure has been proved.

Proof. (2) If it satisfies $m_1 = m_2$, then for $1 \leqslant i \leqslant 2^n - 1$, $m_1(H_i) = m_2(H_i)$.

From the Eq. (11), a conclusion is drawn that $m_{F_1}(H_i) = m_{F_2}(H_i)$. So, it is obvious to conclude the following equation:

$$\begin{aligned} FBD_{SKL}(m_1, m_2) =& \frac{1}{2}\sum_{i=1}^{2^n-1} m_{F_1}(H_i) \log \frac{m_{F_1}(H_i)}{\sqrt{m_{F_1}(H_i) \times m_{F_2}(H_i)}} \\ &+ \frac{1}{2}\sum_{j=1}^{2^n-1} m_{F_2}(H_j) \log \frac{m_{F_2}(H_j)}{\sqrt{m_{F_2}(H_j) \times m_{F_1}(H_j)}} \\ =& 0. \end{aligned}$$

Therefore, it is proved that if $m_1 = m_2$, then $FBD_{SKL}(m_1, m_2) = 0$.

On the other hand, when it satisfies the equation $FBD_{SKL}(m_1, m_2) = 0$, from Proof. (1), it is proved that for $1 \leqslant i \leqslant 2^n - 1$, it is already proved that:

$$\begin{aligned} &\frac{1}{2}\left[m_{F_1}(H_i) \log \frac{m_{F_1}(H_i)}{\sqrt{m_{F_1}(H_i) \times m_{F_2}(H_i)}} \right. \\ &\left. + m_{F_2}(H_i) \log \frac{m_{F_2}(H_i)}{\sqrt{m_{F_2}(H_i) \times m_{F_1}(H_i)}} \right] \\ &= \frac{1}{4}\left(\log m_{F_1}(H_i) - \log m_{F_2}(H_i)\right)\left(m_{F_1}(H_i) - m_{F_2}(H_i)\right) \\ &\geqslant 0. \end{aligned}$$

Thus, in this case, it is further concluded that

$$\frac{1}{4}\left(\log m_{F_1}(H_i) - \log m_{F_2}(H_i)\right)\left(m_{F_1}(H_i) - m_{F_2}(H_i)\right) = 0$$

It is obvious that if this function $\left(\log m_{F_1}(H_i) - \log m_{F_2}(H_i)\right)\left(m_{F_1}(H_i) - m_{F_2}(H_i)\right)$ equals the value of 0, then $m_{F_1}(H_i) = m_{F_2}(H_i)$. Then it can be summarized that $m_{F_1} = m_{F_2}$, so from the Eq. (11), in this case, it is further inferred that $m_1 = m_2$.

Therefore, it is proved that if $FBD_{SKL}(m_1, m_2) = 0$, then $m_1 = m_2$.

Hence, the nondegeneracy of FBD_{SKL} divergence measure has been proved.

Proof. (3) Consider $FBD_{SKL}(m_1, m_2)$:

$$\begin{aligned} FBD_{SKL}(m_1, m_2) =& \frac{1}{2}\sum_{i=1}^{2^n-1} m_{F_1}(H_i) \log \frac{m_{F_1}(H_i)}{\sqrt{m_{F_1}(H_i) \times m_{F_2}(H_i)}} \\ &+ \frac{1}{2}\sum_{j=1}^{2^n-1} m_{F_2}(H_j) \log \frac{m_{F_2}(H_j)}{\sqrt{m_{F_2}(H_j) \times m_{F_1}(H_j)}} \\ =& \frac{1}{2}\sum_{i=1}^{2^n-1} m_{F_2}(H_i) \log \frac{m_{F_2}(H_i)}{\sqrt{m_{F_2}(H_i) \times m_{F_1}(H_i)}} \\ &+ \frac{1}{2}\sum_{j=1}^{2^n-1} m_{F_1}(H_j) \log \frac{m_{F_1}(H_j)}{\sqrt{m_{F_1}(H_j) \times m_{F_2}(H_j)}} \\ =& FBD_{SKL}(m_2, m_1). \end{aligned}$$

Thus, we have $FBD_{SKL}(m_1, m_2) = FBD_{SKL}(m_2, m_1)$.

Hence, the symmetry of FBD_{SKL} is proved.

Proof. (4) Consider H_i in the frame of discernment Θ, then for $H_i \in 2^\Theta$:

If $m_1(H_i) > 0$ or $m_2(H_i) > 0$, then $|H_i| = 1$. Therefore:

$$m_{F_k}(H_i) = \sum_{H_i \subseteq G_i} \frac{m_k(G_i)}{2^{|G_i|} - 1} = \frac{m_k(H_i)}{2^1 - 1} = m_k(H_i), \text{ where } k = 1, 2.$$

Thus, we have:

$$\begin{aligned} FBD_{SKL}(m_1, m_2) =& \frac{1}{2}\sum_{i=1}^{2^n-1} m_{F_1}(H_i) \log \frac{m_{F_1}(H_i)}{\sqrt{m_{F_1}(H_i) \times m_{F_2}(H_i)}} \\ &+ \frac{1}{2}\sum_{j=1}^{2^n-1} m_{F_2}(H_j) \log \frac{m_{F_2}(H_j)}{\sqrt{m_{F_2}(H_j) \times m_{F_1}(H_j)}} \\ =& \frac{1}{2}\sum_{i=1}^{2^n-1} m_1(H_i) \log \sqrt{\frac{m_1(H_i)}{m_2(H_i)}} \\ &+ \frac{1}{2}\sum_{i=1}^{2^n-1} m_2(H_i) \log \sqrt{\frac{m_2(H_i)}{m_1(H_i)}} \\ =& \frac{1}{4}\sum_{i=1}^{2^n-1} m_1(H_i) \log \frac{m_1(H_i)}{m_2(H_i)} \\ &+ \frac{1}{4}\sum_{i=1}^{2^n-1} m_2(H_i) \log \frac{m_2(H_i)}{m_1(H_i)} \\ =& \frac{1}{4}\left(D_{KL}(m_1, m_2) + D_{KL}(m_2, m_1)\right). \end{aligned}$$

Thus, it is proved that under the certain circumstance $\forall |H_i| = 1$, then it is concluded that $FBD_{SKL}(m_1, m_2) = \frac{1}{4}\left(D_{KL}(m_1, m_2) + D_{KL}(m_2, m_1)\right)$.

3.4. Performance of fractal-based belief KL divergence measure

In this section, several examples are provided to evaluate the performance of the symmetric fractal-based belief KL divergence measure.

Note that the value of $FBD_{SKL}(m_1, m_2)$ tends to infinity when fractal assignment value of $\sqrt{m_{F_1}(H_i) \times m_{F_2}(H_i)}$ converges to 0. In this case, this proposed function $FBD_{SKL}(m_1, m_2)$ is not applied. So an extremely small constant number 1×10^{-12} is defined to act as the lower bound of the fractal BPA assignment and replace those values out of this lower bound (even zero) (Guo and Xin, 2005).

Let us return to Example 1, after constructing the fractal evidence functions, the final results are calculated as follows:

$$\begin{aligned} &FBD_{SKL}(m_1, m_3) = 3.3618, \\ &FBD_{SKL}(m_2, m_3) = 14.3125. \end{aligned}$$

In Example 1, according to Fig. 1, it is true that the function pair between m_1 and m_3 is much less conflicting than the pair between m_2 and m_3. Therefore, unlike BJS divergence, symmetric fractal-based belief KL divergence takes the power sets of multisets into consideration.

Then, let us return to Example 2. With the increment of variable α, it is obvious that the conflict between m_1 and m_2 is lowing, and finally, when $\alpha = 1$, m_1 is equivalent to m_2. As shown in Fig. 5, The curve trend of FBD_{SKL}, marked with orange color, is in line with the expected result. Note when m_1 is equivalent to m_2, we have:

$$FBD_{SKL}(m_1, m_2) = 0. \tag{14}$$

Note that in this condition: $m_1 = m_2$, the nondegeneracy property of the symmetric fractal-based belief KL divergence is revealed in Eq. (14).

As for the $\mathfrak{B}$ divergence marked with the blue color, there is a counterintuitive turning point in the curve. And this turning point reveals that the divergence between m_1 and m_2 is not monotone decreasing. This is a departure from our expectation because the m_1 and m_2 should have less conflict as m_1 is increasingly similar to m_2.

So in this case, the proposed symmetric fractal-based belief KL divergence is in line with the trend, while $\mathfrak{B}$ divergence appears to have limitations to reflect the divergence between two BPAs.

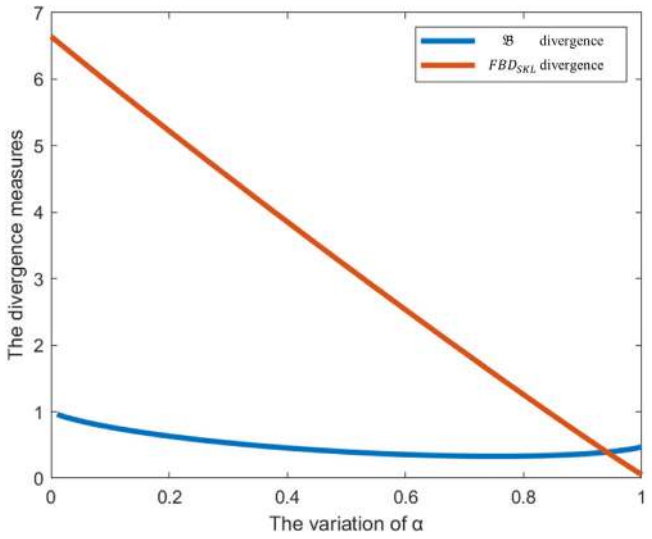

Fig. 5. The divergence measure comparison.

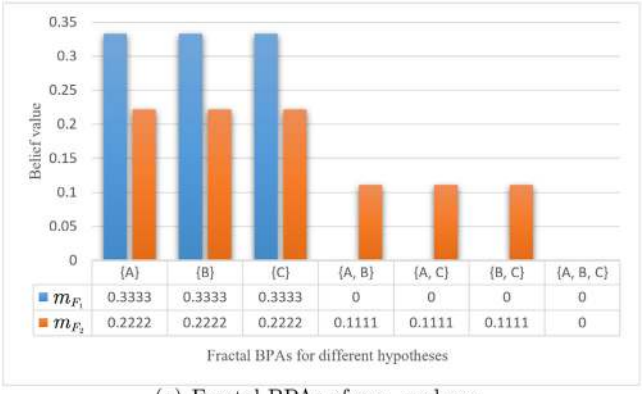

(a) Fractal BPAs of m_{F_1} and m_{F_2}

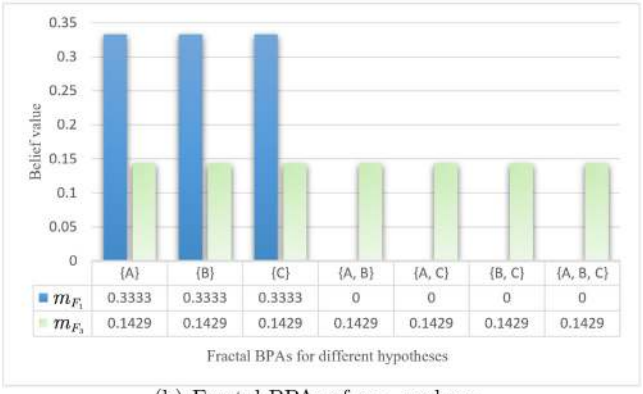

(b) Fractal BPAs of m_{F_1} and m_{F_3}

Fig. 6. The comparisons between fractal functions . (a) Fractal BPAs of m_{F_1} and m_{F_2}. (b) Fractal BPAs of m_{F_1} and m_{F_3}.

Example 3. Suppose that there are three independent BPAs m_1, m_2 and m_3 in the frame of discernment $\Theta = \{A, B, C\}$:

$m_1\{A\} = \frac{1}{3}$, $m_1\{B\} = \frac{1}{3}$, $m_1\{C\} = \frac{1}{3}$;
$m_2\{A, B\} = \frac{1}{3}$, $m_2\{A, C\} = \frac{1}{3}$, $m_2\{B, C\} = \frac{1}{3}$;
$m_3\{A, B, C\} = \frac{1}{3}$.

According to Eq. (11), the m_{F_1}, m_{F_2} and m_{F_3} are calculated, respectively. Then, the divergence value comparisons between m_{F_1} and m_{F_2}, as well as comparisons between m_{F_1} and m_{F_3} are shown in Fig. 6(a) and (b), respectively. It is clearly noticed that conflict between m_{F_1} and m_{F_2} is less than conflict between m_{F_1} and m_{F_3}. The proposed FBD_{SKL} measure is implemented to quantify the conflict of these two pairs of BPAs. Finally, the results are obtained:

$$FBD_{SKL}(m_1, m_2) = 3.1065,$$
$$FBD_{SKL}(m_1, m_3) = 5.4683.$$

Hence, we have:

$$FBD_{SKL}(m_1, m_2) < FBD_{SKL}(m_1, m_3).$$

This consequence is in line with expectations. By splitting the BPA through a fractal process, the proposed symmetric fractal-based belief KL divergence is effective in measuring the conflict between BPAs.

4. A novel FBD_{SKL}-based multi-source data fusion algorithm

In this section, the symmetric fractal-based belief KL divergence model is applied in multi-source data fusion. Thus, the FBD_{SKL}-based multi-source data fusion (FBD_{SKL}-MSDF) algorithm is proposed. The specific algorithm steps are shown in detail as follows and a flowchart of the FBD_{SKL}-MSDF algorithm is shown in Fig. 7.

Step 1: The proposed FBD_{SKL} measure between two arbitrary BPAs, m_i and m_j $(i, j = 1, 2, \ldots, N)$ each of which contains n mutually exclusive events, is implemented in Eq. (13). The conflict measure matrix (CMM) composed with the FBD_{SKL} divergence between m_i and m_j is constructed as follows:

$$CMM = \begin{bmatrix} 0 & FBD_{SKL_{12}} & \cdots & FBD_{SKL_{1N}} \\ FBD_{SKL_{21}} & 0 & \cdots & FBD_{SKL_{2N}} \\ \vdots & \vdots & \ddots & \vdots \\ FBD_{SKL_{N1}} & FBD_{SKL_{N2}} & \cdots & 0 \end{bmatrix}. \tag{15}$$

Step 2: Then, a similarity measure matrix (SMM) is constructed by the normalization method.

$$SMM = \begin{bmatrix} 1 & S_{12} & \cdots & S_{1N} \\ S_{21} & 1 & \cdots & S_{2N} \\ \vdots & \vdots & \ddots & \vdots \\ S_{N1} & S_{N2} & \cdots & 1 \end{bmatrix}, \tag{16}$$

where $S_{ij} = \frac{\max\left(FBD_{SKL_{ij}}\right) - FBD_{SKL_{ij}}}{\max\left(FBD_{SKL_{ij}}\right) - \min\left(FBD_{SKL_{ij}}\right)}$ and S_{ii} is defined with constant value 1, which temporarily explains the self-similarity, however, is ignored in the following steps.

Step 3: The total calculated supporting value of every piece of evidence is summed up by the elements which describe the extent of favoring each other in the SMM. And this supporting value $Sup(m_i)$ is defined as:

$$Sup(m_i) = \sum_{j=1, j\neq i}^{N} e^{S_{ij}}. \tag{17}$$

Step 4: After calculating the total supporting value $Sup(m_i)$ of each BPA, the credit value of every BPA, Crd_i, is obtained by the $Sup(m_i)$ proportion:

$$Crd_i = \frac{Sup(m_i)}{\sum_{i=1}^{N} Sup(m_i)}. \tag{18}$$

Step 5: On the basis of the normalized supporting value Crd_i, the initial evidence is averaged with this weight Crd_i. And the new BPA $\tilde{m}$ is calculated:

$$\tilde{m} = \sum_{i=1}^{N} (Crd_i \times m_i). \tag{19}$$

Step 6: The newly averaged BPA $\tilde{m}$ is merged with $N-1$ times by Dempster's combination rule:

$$Fin(\tilde{m}) = \left(\left(\left(\left(\tilde{m} \oplus \tilde{m}\right)_1 \oplus \tilde{m}\right)_2 \oplus \ldots\right)_{N-2} \oplus \tilde{m}\right)_{N-1}. \tag{20}$$

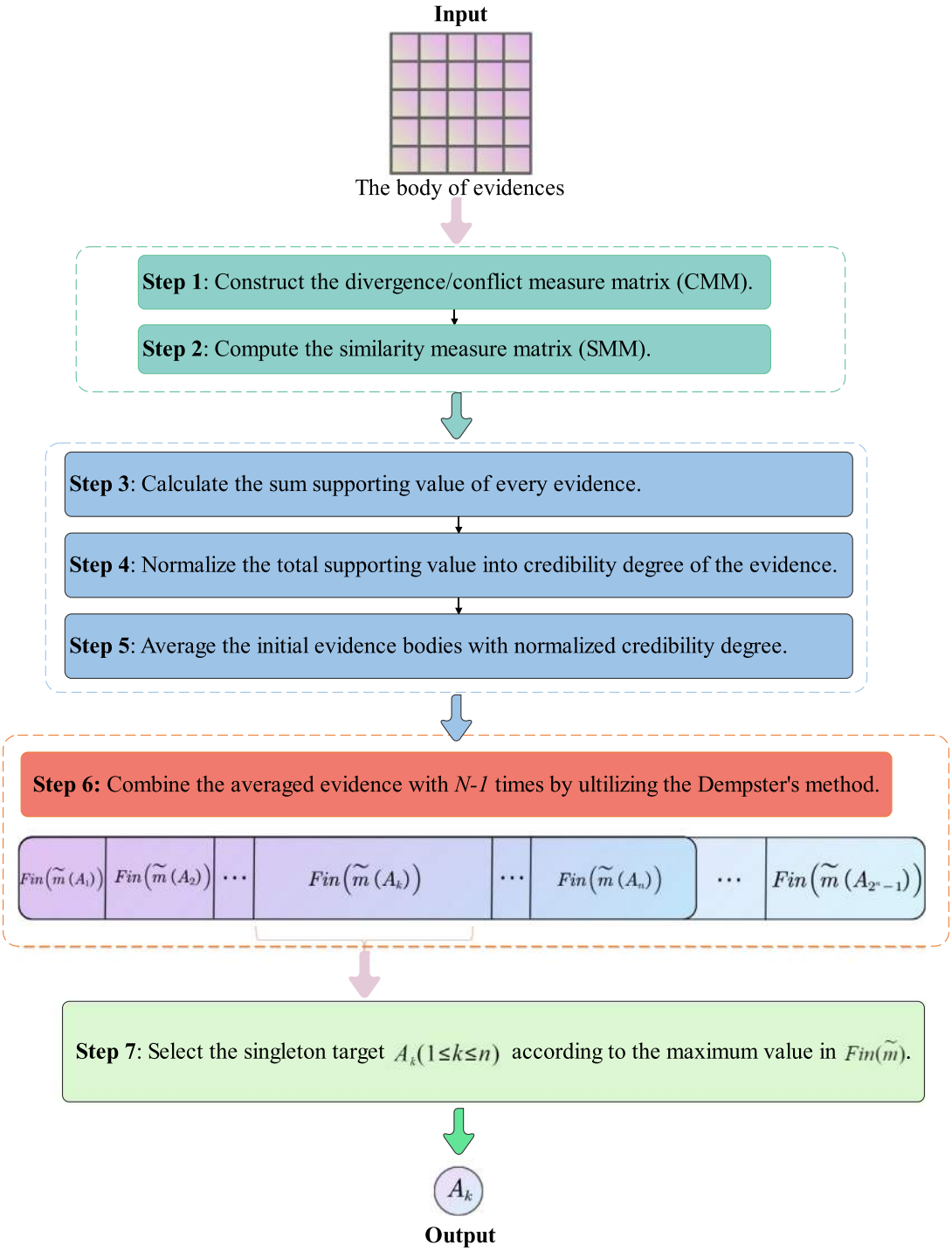

Fig. 7. The flowchart of FBD_{SKL}-MSDF algorithm.

Step 7: Based on the final fusion consequence, the highest singleton-supporting value in $Fin\left(\widetilde{m}\right)$ infers the target event A_k $(1 \leqslant k \leqslant n)$, that is:

$$A_k \leftarrow \max_{1\leqslant i\leqslant n} \left\{ Fin\left(\widetilde{m}\left(A_i\right)\right)\right\}. \tag{21}$$

The whole procedures of FBD_{SKL}-MSDF are summarized into pseudocode in Algorithm 1. Now we analyze the complexity of the proposed FBD_{SKL}-MSDF method. The time complexity and space complexity of each step are analyzed as shown in Table 1.

First, the time complexity of the algorithm is analyzed in detail. Step 1 is the operation to construct the CMM by calculating the FBD_{SKL} divergence in each pair of evidences, this operation consumes $\mathcal{O}(N^2)\times \mathcal{O}(2^n)$ in time complexity and $\mathcal{O}(N^2)\times\mathcal{O}(2^n)$ in space complexity. Step 2 transforms CMM into SMM, and consumes $\mathcal{O}(N^2)$ in time complexity and $\mathcal{O}(N^2)\times\mathcal{O}(2^n)$ in space complexity. Step 3 calculates the sum of supporting values, and consumes $\mathcal{O}(N^2)$ in time complexity and $\mathcal{O}(N)$ in space complexity. Based on the sum of supporting values, step 4 allocates the credit value to each BPA, and it consumes $\mathcal{O}(N)$ in time complexity and $\mathcal{O}(N)$ in space complexity. Step 5 averages the BPAs into $\widetilde{m}$, and this consumes $\mathcal{O}(N)$ in time complexity and $\mathcal{O}(1)\times\mathcal{O}(2^n)$ in space complexity. Finally, step 6 implements the Dempster's rule $n-1$ times, and this consumes $\mathcal{O}(N)\times\mathcal{O}(2^n)$ in time complexity and

Algorithm 1: A novel FBD_{SKL}-MSDF algorithm

Input: A set of evidence functions $m = \{m_1, m_2, ..., m_i, m_j, ..., m_N\}$ (every BPA contains n mutually exclusive events);
Output: Supporting event according to fusion results;

```
for i = 1; i ⩽ N do
    for j = 1; j ⩽ N do
        Compute the divergence FBD_SKL(m_i, m_j) using Eq. (13);
    end
end
Construct the conflict measure matrix CMM using Eq. (15);
Compute the similarity measure matrix SMM using Eq. (16);
for i = 1; i ⩽ N do
    Calculate the Sup_i of every BPA using Eq. (17);
end
for i = 1; i ⩽ N do
    Normalize the Sup_i into Crd_i weights using Eq. (18);
end
for i = 1; i ⩽ N do
    With Crd_i weights, average the initial BPAs into m̃ using Eq. (19);
end
for i = 1; i ⩽ N − 1 do
    Combine the m̃ with N − 1 times through Dempster's method into Fin(m̃) using Eq. (20);
end
Select the target event A_k (1 ⩽ k ⩽ n) based on the highest singleton-supporting value from Fin(m̃) using Eq. (21);
```

Table 1
The time and space complexity in the FBD_{SKL}-MSDF algorithm.

Steps	Time complexity	Space complexity	Description
Step 1	$\mathcal{O}(N^2)\times\mathcal{O}(2^n)$	$\mathcal{O}(N^2)\times\mathcal{O}(2^n)$	Construct the CMM by calculating FBD_{SKL}
Step 2	$\mathcal{O}(N^2)$	$\mathcal{O}(N^2)\times\mathcal{O}(2^n)$	Transform CMM into SMM
Step 3	$\mathcal{O}(N^2)$	$\mathcal{O}(N)$	Calculate the sum of supporting values of each BPA
Step 4	$\mathcal{O}(N)$	$\mathcal{O}(N)$	Allocate the credit value to each BPA
Step 5	$\mathcal{O}(N)$	$\mathcal{O}(1)\times\mathcal{O}(2^n)$	Average the BPAs into $\widetilde{m}$
Step 6	$\mathcal{O}(N)\times\mathcal{O}(2^n)$	$\mathcal{O}(1)\times\mathcal{O}(2^n)$	Combine $\widetilde{m}$ with Dempster's rule
Overall	$\mathcal{O}(N^2)\times\mathcal{O}(2^n)$	$\mathcal{O}(N^2)\times\mathcal{O}(2^n)$	Computation complexity

Explanation of notations.
n : the size of frame of discernment Θ;
N : the number of BPAs to combine.

$\mathcal{O}(1)\times\mathcal{O}(2^n)$ in space complexity. Thus, the overall time complexity of the FBD_{SKL}-MSDF algorithm is $\mathcal{O}(N^2)\times\mathcal{O}(2^n)$ and overall space complexity of the FBD_{SKL}-MSDF algorithm is $\mathcal{O}(N^2)\times\mathcal{O}(2^n)$.

As for the other methods: Dempster's algorithm and Murphy's algorithm take $\mathcal{O}(N)\times\mathcal{O}(2^n)$ in time complexity and $\mathcal{O}(2^n)$ in space complexity, because they do not construct the matrix like CMM or SMM to reflect the relationship between two BPAs; Deng et al.'s, BJS divergence and $\mathfrak{B}$ divergence algorithms expense the same with our FBD_{SKL}-MSDF algorithm: $\mathcal{O}(N^2)\times\mathcal{O}(2^n)$ in time complexity and $\mathcal{O}(N^2)\times\mathcal{O}(2^n)$ in space complexity. In general, computational complexity comparisons among these methods can be intuitively seen in Table 2. Although Dempster's algorithm and Murphy's algorithm reveal less time consumption, these algorithms listed in Table 2, are applied in numeric examples and applications, thus their performance is discussed in Sections 5 and 6.

Table 2
The computational complexity comparison among different algorithms.

Algorithm	Time complexity	Space complexity
Dempster	$\mathcal{O}(N)\times\mathcal{O}(2^n)$	$O(2^n)$
Murphy	$\mathcal{O}(N)\times\mathcal{O}(2^n)$	$O(2^n)$
Deng et al.	$\mathcal{O}(N^2)\times\mathcal{O}(2^n)$	$\mathcal{O}(N^2)\times\mathcal{O}(2^n)$
BJS divergence	$\mathcal{O}(N^2)\times\mathcal{O}(2^n)$	$\mathcal{O}(N^2)\times\mathcal{O}(2^n)$
$\mathfrak{B}$ divergence	$\mathcal{O}(N^2)\times\mathcal{O}(2^n)$	$\mathcal{O}(N^2)\times\mathcal{O}(2^n)$
FBD_{SKL}-MSDF	$\mathcal{O}(N^2)\times\mathcal{O}(2^n)$	$\mathcal{O}(N^2)\times\mathcal{O}(2^n)$

Table 3
BPA with their belief values.

BPA	$\{A\}$	$\{B\}$	$\{C\}$	$\{A,C\}$
m_1	0.50	0.08	0.30	0.12
m_2	0.60	0.09	0.01	0.30
m_3	0.43	0.06	0.01	0.50
m_4	0.01	0.40	0.38	0.21
m_5	0.40	0.19	0.01	0.40

5. Experiments

In this section, a concrete recognition experiment with multi-source is conducted to analyze the performance of FBD_{SKL}-MSDF algorithm. Then, a sensitivity analysis is implemented to verify the robustness of this FBD_{SKL}-MSDF algorithm. Experimental data based on data set (Deng et al., 2004) are used for comparison among existing methods. To make our conclusion convincing, the classic multi-source fusion algorithms of Dempster (2008), Deng et al. (2004) and Murphy (2000) are first taken into account. Furthermore, the noted and existing divergence-based multi-source fusion algorithms, including BJS divergence and $\mathfrak{B}$, are introduced in Section 2. A further overall performance analysis among them with the proposed FBD_{SKL}-MSDF method is conducted in this section and the application section.

5.1. Problem statement

Suppose there are three singleton target hypotheses $\{A\}$, $\{B\}$, and $\{C\}$ in the frame of discernment Θ. Additionally, in Table 3, there are five BPAs m_1, m_2, m_3, m_4 and m_5 given to help us to make a decision of the final supporting target.

5.2. Implementation of FBD_{SKL}-MSDF algorithm

Step 1: Construct the conflict measure matrix (CMM) as follows:

$$CMM = \begin{bmatrix} 0 & 0.0893 & 0.0748 & 0.3603 & 0.0944 \\ 0.0893 & 0 & 0.0236 & 0.5742 & 0.0346 \\ 0.0748 & 0.0236 & 0 & 0.5056 & 0.0428 \\ 0.3603 & 0.5742 & 0.5056 & 0 & 0.3520 \\ 0.0944 & 0.0346 & 0.0428 & 0.3520 & 0 \end{bmatrix}.$$

Step 2: Convert constructed CMM above into a similarity measure matrix (SMM) as follows:

$$SMM = \begin{bmatrix} 1 & 0.8806 & 0.9070 & 0.3886 & 0.8714 \\ 0.8806 & 1 & 1.0000 & 0 & 0.9800 \\ 0.9070 & 1.0000 & 1 & 0.1245 & 0.9650 \\ 0.3886 & 0 & 0.1245 & 1 & 0.4036 \\ 0.8714 & 0.9800 & 0.9650 & 0.4036 & 1 \end{bmatrix}.$$

Step 3: Calculate the summed supporting value of every BPA as follows:

$$Sup(m_1) = 8.7546,$$
$$Sup(m_2) = 8.7951,$$
$$Sup(m_3) = 8.9527,$$
$$Sup(m_4) = 5.1047,$$
$$Sup(m_5) = 9.1767.$$

Table 4
Results generated by different methods.

Method	$\{A\}$	$\{B\}$	$\{C\}$	$\{A,C\}$	Target
Dempster (2008)	0.8480	0.0003	0.1374	0.0143	A
Murphy (2000)	0.8971	0.0007	0.0871	0.0152	A
Deng et al. (2004)	0.9230	0.0004	0.0625	0.0142	A
BJS divergence (Xiao, 2019)	0.9234	0.0004	0.0620	0.0143	A
$\mathfrak{B}$ divergence (Xiao, 2020)	0.9184	0.0005	0.0636	0.0175	A
Proposed method	0.9328	0.0003	0.0533	0.0136	A

Table 5
Mean recognition rates and variances generated by different methods.

Method	Mean	Variance	Target
Dempster (2008)	0.8528	1.549×10^{-5}	A
Murphy (2000)	0.8958	0.630×10^{-5}	A
Deng et al. (2004)	0.9183	0.468×10^{-5}	A
BJS divergence (Xiao, 2019)	0.9030	0.613×10^{-5}	A
$\mathfrak{B}$ divergence (Xiao, 2020)	0.9274	0.453×10^{-5}	A
Proposed method	0.9363	0.386×10^{-5}	A

Step 4: Normalize the calculated sum degrees as credit weights of every BPA as follows:

$$Crd\left(m_1\right) = 0.2147,$$
$$Crd\left(m_2\right) = 0.2157,$$
$$Crd\left(m_3\right) = 0.2195,$$
$$Crd\left(m_4\right) = 0.1251,$$
$$Crd\left(m_5\right) = 0.2250.$$

Step 5: Average the initial BPAs into $\widetilde{m}$ as follows:

$$\widetilde{m}(\{A\}) = 0.4244,$$
$$\widetilde{m}(\{B\}) = 0.1426,$$
$$\widetilde{m}(\{C\}) = 0.1185,$$
$$\widetilde{m}(\{A,C\}) = 0.3165.$$

Step 6: Combine the averaged BPA $\widetilde{m}$ with $n-1$ times and get the final answer $Fin\left(\widetilde{m}\right)$ as shown in Fig. 8 and Table 4:

Step 7: Select the objective A as the target event.

As shown in Table 4, it is noticed that event A is recognized as the target with distinct recognition values according to the proposed FBD_{SKL}-MSDF algorithm and the other five well-known related algorithms. Specifically, Dempster's method recognizes the target A with relatively lowest belief value of 0.8480 among the four methods. This consequence may be caused by m_5 that is highly conflicting with the other four BPAs. However, Dempster's method could not appropriately cope with these highly conflicting BPAs. As a relatively marked improvement in the recognition value, Murphy's method recognizes the target A with a belief value of 0.8971 by implementing a numerical average of BPA. Deng et al.'s method recognizes the target A with a higher belief value of 0.9230. As for belief-based divergence algorithms, the target recognition values of BJS divergence method and $\mathfrak{B}$ are 0.9234 and 0.9184, relatively. As is introduced in Examples 1 and 2, their performance may be restricted in some cases. FBD_{SKL}-MSDF method recognizes the target A with the highest belief value of 0.9328. From Fig. 8, the recognition value is presented in a visualized way: the highest accuracy indicates the proposed FBD_{SKL}-MSDF method could appropriately handle the highly conflicting and effectively recognize the correct target in multi-source data fusion.

5.3. Sensitivity analysis

In this section, a sensitivity analysis is conducted to validate the superiority and robustness of the proposed FBD_{SKL}-MSDF algorithm. To accomplish this sensitivity analysis, white Gaussian noise with a square deviation of 0.01 is added to the belief value of event $\{A\}$ in every BPA. After that, every BPA is normalized with a total belief value of 1. And multi-source fusion algorithms, including Dempster's method, Murphy's method, Deng et al.'s method, BJS divergence method, $\mathfrak{B}$ divergence method and FBD_{SKL}-MSDF method, are implemented. Repeating this whole process with 100 times, the varying recognition values of event $\{A\}$ are shown in Fig. 9, accompanied with its box chart of recognition values in Fig. 9(a) and histogram of variances in Fig. 9(b).

From Table 5, after conducting 100 times of experiments, all methods recognize the target A with obviously distinct values. Dempster's method obtains the lowest mean recognition value of 0.8528, because it cannot handle the conflict BPAs. Murphy's method has higher accuracy than Dempster's method and obtains the mean recognition value of 0.8958. The accuracy promotion seems obvious because Murphy's method conducts a numerical average preprocessing algorithm. However, this averaging algorithm does not perfectly work out the conflict between BPAs, for it does not take the discrepancy of BPAs into consideration as well. As an accuracy promotion in Deng et al.'s method, it obtains the mean recognition value of 0.9183. Introducing the distance measure matrix, this method has a higher recognition value than these previous methods. As for the BJS divergence method and $\mathfrak{B}$ divergence method, they obtain the mean recognition value of 0.9030 and 0.9274, relatively. Despite the apparent improvement in accuracy by Deng et al.'s method, by contrast, the proposed FBD_{SKL}-MSDF algorithm method obtains the highest mean recognition value of 0.9363.

To analyze the sensitivity of each method, white Gaussian noise with a square deviation of 0.01 is added to the belief value of event $\{A\}$ in every BPA. So, the recognition value of target $\{A\}$ corresponding to every experiment is shown in Fig. 9.

Based on recognition values from 100 times of experiments, the distribution and variance of recognition values reflect sensitivity of its model. From the box chart in Fig. 9(a), the discrete distribution of data can be described in a visualized way, because the interval box between the lower quartile and upper quartile represents the main data aggregation range. Intuitively, it is noticed that the recognition value of the proposed FBD_{SKL}-MSDF algorithm is relatively densely distributed with fewer outliers. And From the histogram of variances in Fig. 9(b), the variance value is further directly displayed. The variance values of six methods of Dempster, Murphy, Deng et al. BJS divergence, $\mathfrak{B}$ divergence and the proposed FBD_{SKL}-MSDF algorithm, present with: 1.549×10^{-5}, 0.630×10^{-5}, 0.468×10^{-5}, 0.613×10^{-5}, 0.453×10^{-5}, 0.386×10^{-5}.

As a comparison among the three divergence algorithms: BJS divergence method gets the lowest accuracy and the highest variance; there are some performance improvements of $\mathfrak{B}$ divergence in its higher accuracy and lower variance, but there are more outliers from Fig. 9(a) than other methods; FBD_{SKL}-MSDF algorithm performs best with the highest mean recognition value and the lowest variance. To draw a conclusion in this case, by introducing fractal process and KL divergence, even with varying BPAs caused by the Gaussian noise, it is concluded that the FBD_{SKL}-MSDF algorithm indeed reveals its highest accuracy and robustness among the four methods as shown in Fig. 9 and Table 5.

6. Application

In this section, the proposed FBD_{SKL}-MSDF algorithm is applied in two practical classification problems.

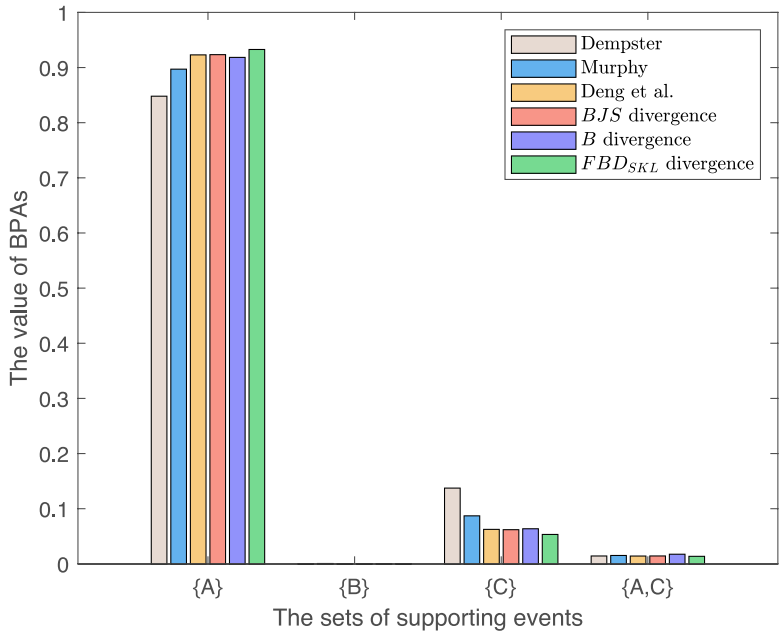

Fig. 8. Results bar generated by different methods.

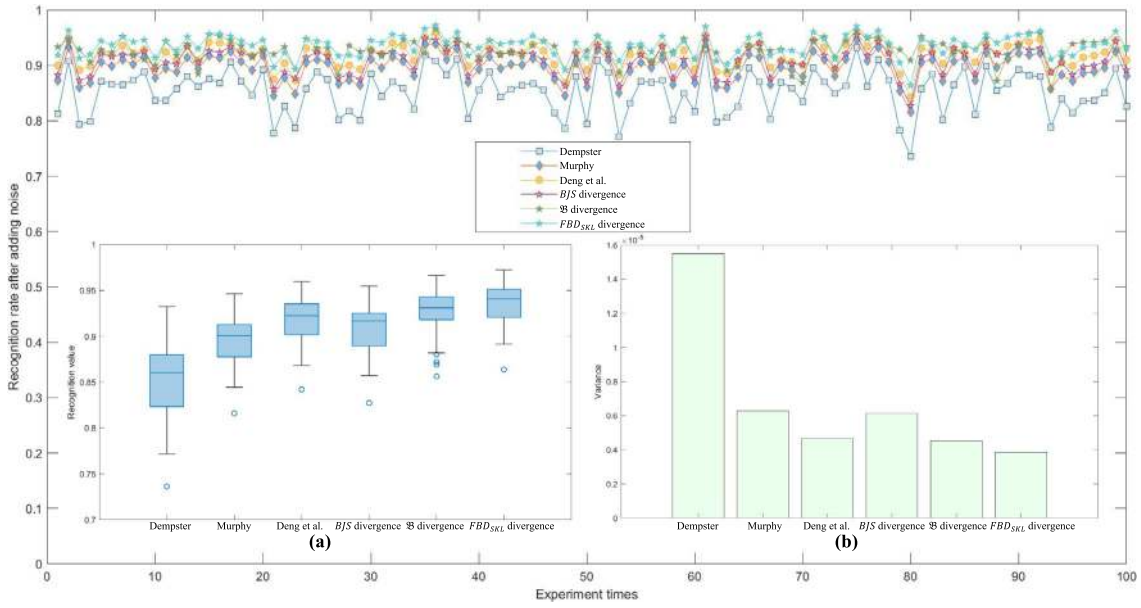

Fig. 9. Sensitivity analysis generated by different methods. (a) Box chart of recognition values of different methods. (b) Histogram of variances of different methods.

Firstly, the Iris and mammographic datasets are both obtained from the UCI machine learning repository.[1]

Each dataset is comprised of p properties. And each dataset is categorized into n types. For every type in one dataset, the data portion of 60% are randomly selected as training dataset, and the other 40% are selected as test dataset. Based on the models constructed with training data, the BPAs generated by the corresponding properties are given. In the recognition decision step, multi-source fusion algorithms including Dempster's method (Dempster, 2008), Murphy's method (Murphy, 2000), Deng et al.'s method (Deng et al., 2004), BJS divergence (Xiao, 2019), $\mathfrak{B}$ divergence (Xiao, 2020) and the proposed FBD_{SKL}-MSDF method are implemented, respectively. A generalized process comprised of the model-training and multi-source fusion is described in Fig. 10. This process is repeated 100 times. In every single process, the training data are reselected randomly, while the rest of the raw data are labeled as the testing data.

Then, the recognition application is conducted with the Iris dataset, which is comprised of 4 properties: sepal length, sepal width, petal length and petal width. And Iris dataset can be categorized into 3 types of irises: Setosa, Versicolor and Virginica, each of which has 50 samples.

From Table 6, the recognition rates of methods of Dempster, Murphy, Deng et al. BJS divergence, $\mathfrak{B}$ divergence and the proposed FBD_{SKL}-MSDF method are separately displayed. In this classification application: Dempster's method obtains the mean accuracy of 0.9060; Murphy's method obtains the mean accuracy of 0.9223; Deng et al.'s method obtains the mean accuracy of 0.9355; BJS divergence obtains the mean accuracy of 0.9222, $\mathfrak{B}$ divergence obtains the mean accuracy of 0.9288; the proposed FBD_{SKL}-MSDF method obtains the mean

[1] http://archive.ics.uci.edu/ml/datasets/.

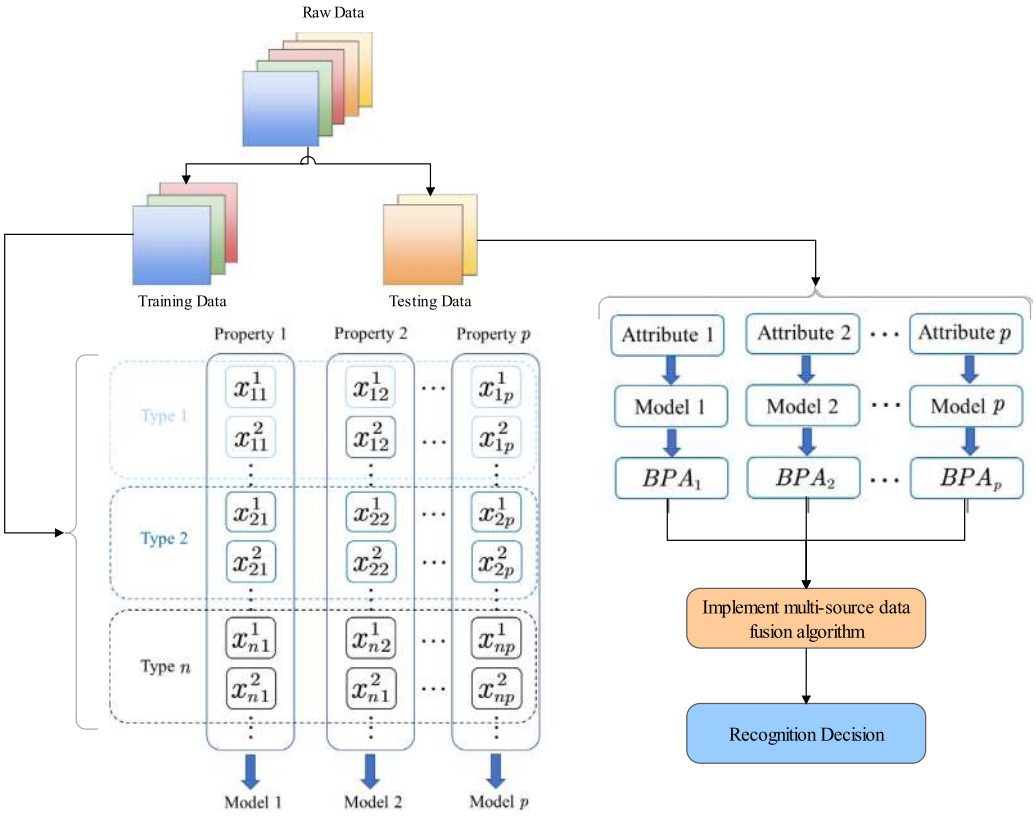

Fig. 10. The flowchart of experiment process.

Table 6
Mean recognition rates generated by different methods on Iris dataset.

Method	Mean recognition rate
Dempster (2008)	0.9060
Murphy (2000)	0.9223
Deng et al. (2004)	0.9335
BJS divergence (Xiao, 2019)	0.9222
$\mathfrak{B}$ divergence (Xiao, 2020)	0.9288
Proposed method	0.9408

Table 7
Mean recognition rates generated by different methods on mammographic dataset.

Method	Mean recognition rate
Dempster (2008)	0.8573
Murphy (2000)	0.8565
Deng et al. (2004)	0.8714
BJS divergence (Xiao, 2019)	0.8867
$\mathfrak{B}$ divergence (Xiao, 2020)	0.8771
Proposed method	0.8990

accuracy of 0.9408. Shown in Fig. 11, it is directly observed that the proposed FBD_{SKL}-MSDF method performs better than the three existing well-known methods of Dempster, Murphy and Deng et al. and two recently proposed belief divergence methods BJS divergence and $\mathfrak{B}$ divergence.

It is relatively simple with the limitation in dimension and the number of samples of the Iris dataset. Further, we consider applying the multi-source data fusion algorithms in the classification of the mammographic dataset obtained from the UCI machine learning repository. To stress the significance of this application, we could make a decision on the severity (benign or malignant breast cancer) based on the obtained five attributes: BI-RADS (Breast Imaging Reporting and Data System) assessment, age, shape, margin and density. There are 516 benign medical samples and 445 malignant medical samples to study.

Except for the higher dimension in the dataset attributes and more quantity in the samples, the experiment process is the same as the one on the Iris dataset. From Table 7, the recognition rates of methods of Dempster, Murphy, Deng et al. BJS divergence, $\mathfrak{B}$ divergence and the proposed FBD_{SKL}-MSDF method are separately displayed. In addition to the exact mean accuracy, it is directly observed from Fig. 12 that the proposed FBD_{SKL}-MSDF method performs better than the three existing well-known methods of Dempster, Murphy and Deng et al. and two recently proposed belief divergence methods BJS divergence and $\mathfrak{B}$ divergence.

In conclusion, the proposed FBD_{SKL}-MSDF method is well applied in the practical application according to its performance on the Iris dataset and the mammographic dataset.

7. Conclusion

In this study, combined with a fractal preprocess with KL divergence, a new divergence measure intended called FBD_{SKL} for evidence theory is proposed, which effectively measures mutual conflict between given BPAs. The study's key contribution is that the generalization model based on KL divergence: FBD_{SKL}, with desirable properties including nonnegativity, nondegeneracy, symmetry and KL-equivalence, is a well-constructed model, which makes it well applied in a great diversity of conditions. Furthermore, when the divergence measure between BPAs is quantified, the proposed FBD_{SKL} further takes the overlap-relationship between subsets of BPAs into consideration, which positively influences the performance of a measure. In addition, a multi-source data fusion algorithm based on the proposed belief divergence measure FBD_{SKL}, is developed and is called as FBD_{SKL}-MSDF algorithm. By conducting an experiment and sensitivity analysis on this proposed FBD_{SKL}-MSDF algorithm compared with the well-known existing methods, its superiority and robustness are validated, respectively, corresponding to the higher mean recognition rate and its lower variance. Finally, it is verified that the proposed FBD_{SKL}-MSDF

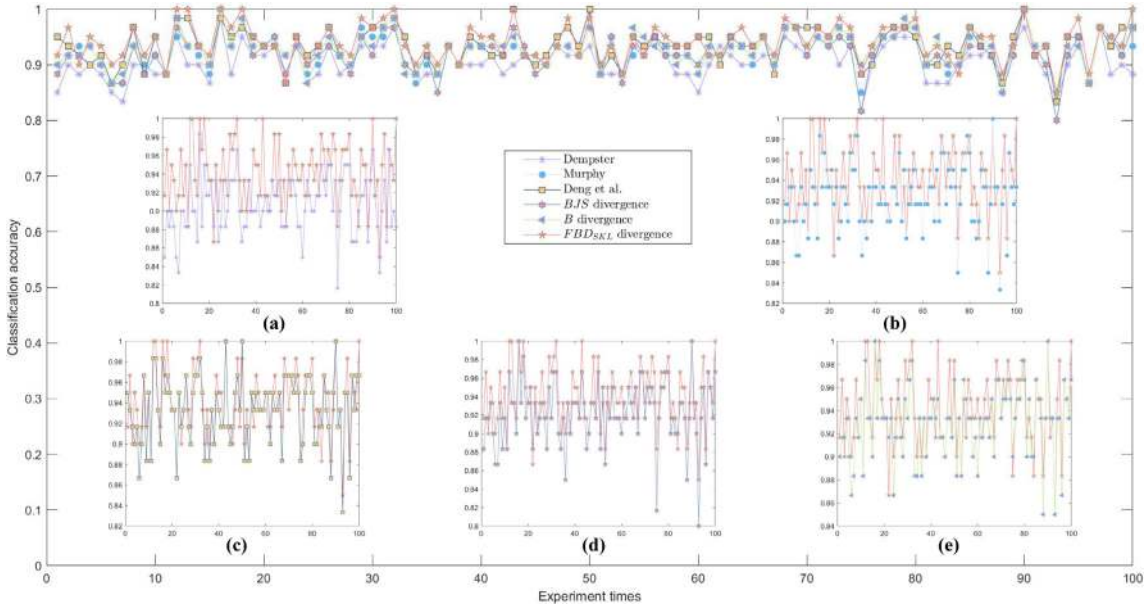

Fig. 11. Recognition rates for target produced by different methods on Iris dataset. (a) Results of Dempster's method and the proposed method. (b) Results of Murphy's method and the proposed method. (c) Results of Deng et al.'s method and the proposed method. (d) Results of BJS divergence method and the proposed method. (e) Results of $\mathfrak{B}$ divergence method and the proposed method.

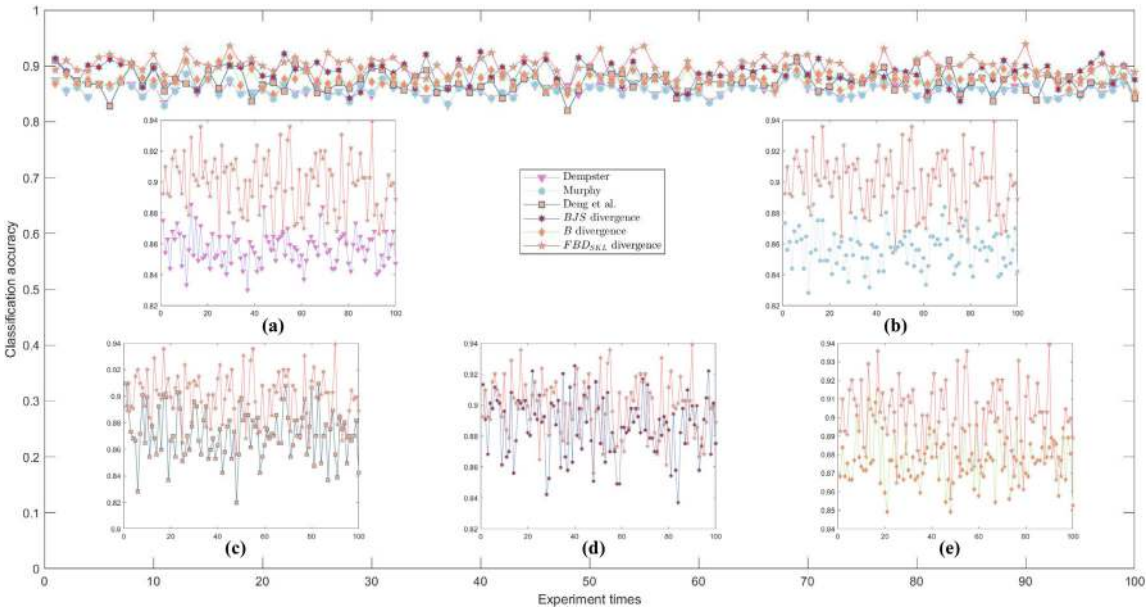

Fig. 12. Recognition rates for target produced by different methods on a mammographic dataset. (a) Results of Dempster's method and the proposed method. (b) Results of Murphy's method and the proposed method. (c) Results of Deng et al.'s method and the proposed method. (d) Results of BJS divergence method and the proposed method. (e) Results of $\mathfrak{B}$ divergence method and the proposed method.

algorithm outperforms the noted existing methods in a real-world application. Based on the above, the proposed FBD_{SKL} fills the gap in the limitation of inappropriate handling between BPAs in the former methods.

In spite of the superior performance in higher accuracy and stronger robustness in the FBD_{SKL}-MSDF algorithm, there still exists weakness below: As is discussed in the computational complexity in FBD_{SKL}-MSDF algorithm in Section 4, the time and space consumption of FBD_{SKL}-MSDF algorithm can reach $\mathcal{O}(N^2) \times \mathcal{O}(2^n)$. This exponential level is noticeable because a great deal of time and space may be consumed if the numbers of BPAs reach large.

Based on the analyzed weakness, the future work can be firstly focused on efficiency improvement. On the one hand, as for the time complexity from Table 1, it is noticed that the construction of CMM consumes the maximum amount of time in the FBD_{SKL}-MSDF algorithm. Every element in CMM needs to calculate the divergence. To improve the calculation efficiency, the proposed FBD_{SKL} measure can be combined with quantum computing to make the computational process parallelable. On the other hand, as for the space complexity, the CMM and SMM are actually redundant in their matrix structure. The symmetric part is a copy of the original element. To address this problem, a better data structure may be put forward to store the divergence value. Furthermore, from Table 2, the time and space

complexity of the existing belief divergence algorithms including BJS divergence and $\mathfrak{B}$ divergence reach $\mathcal{O}(N^2) \times \mathcal{O}(2^n)$. Thus, to apply these divergence measure methods to more complex applications (for instance, the dimension and the number of samples have markedly increased), the algorithm efficiency is urgent to improve. In addition, in future work, we may also apply the proposed FBD_{SKL} measure in the complex field, which can make it a generalized method both in the real number domain and the complex number domain.

CRediT authorship contribution statement

Jie Zeng: Validation, Writing – original draft. **Fuyuan Xiao:** Methodology.

Declaration of competing interest

The authors declare that they have no known competing financial interests or personal relationships that could have appeared to influence the work reported in this paper.

Data availability

No data was used for the research described in the article.

Acknowledgments

The authors greatly appreciate the reviewers' valuable suggestions and the editor's great encouragement. This research is supported by the National Natural Science Foundation of China (No. 62003280), Chongqing Talents: Exceptional Young Talents Project (No. cstc2022ycjh-bgzxm0070), Natural Science Foundation of Chongqing, China (No. CSTB2022NSCQ-MSX0531), and Chongqing Overseas Scholars Innovation Program (No. cx2022024).

References

Cao, Z., Chuang, C.-H., King, J.-K., Lin, C.-T., 2019. Multi-channel EEG recordings during a sustained-attention driving task. Sci. Data 6 (1), 1–8.

Chang, L., Zhang, L., Fu, C., Chen, Y.-W., 2022. Transparent digital twin for output control using belief rule base. IEEE Trans. Cybern. 52 (10), 10364–10378.

Chen, X., Deng, Y., 2022. An evidential software risk evaluation model. Mathematics 10 (13), 2325.

Chen, L., Deng, Y., Cheong, K.H., 2021. Probability transformation of mass function: A weighted network method based on the ordered visibility graph. Eng. Appl. Artif. Intell. 105, 104438.

Chu, C., Li, Y., Liu, J., Hu, S., Li, X., Wang, Z., 2022. A formal model for multiagent Q-learning dynamics on regular graphs. In: Proceedings of the Thirty-First International Joint Conference on Artificial Intelligence, IJCAI. pp. 194–200.

Cui, H., Zhou, L., Li, Y., Kang, B., 2022. Belief entropy-of-entropy and its application in the cardiac interbeat interval time series analysis. Chaos Solitons Fractals 155, 111736.

Dempster, A.P., 1967. Upper and lower probabilities induced by a multivalued mapping. Ann. Math. Stat. 325–339.

Dempster, A.P., 2008. Upper and lower probabilities induced by a multivalued mapping. In: Classic Works of the Dempster-Shafer Theory of Belief Functions. Springer, pp. 57–72.

Deng, Y., 2020a. Information volume of mass function. Int. J. Comput. Commun. Control 15 (6), 3983.

Deng, Y., 2020b. Uncertainty measure in evidence theory. Sci. China Inf. Sci. 63 (11), 1–19.

Deng, Y., 2022. Random permutation set. Int. J. Comput. Commun. Control 17 (1), 4542.

Deng, X., Cui, Y., 2021. An improved belief structure satisfaction to uncertain target values by considering the overlapping degree between events. Inform. Sci. 580, 398–407.

Deng, J., Deng, Y., 2022. Maximum entropy of random permutation set. Soft Comput. http://dx.doi.org/10.1007/s00500--022--07351--x.

Deng, Y., Shi, W., Zhu, Z., Liu, Q., 2004. Combining belief functions based on distance of evidence. Decis. Support Syst. 38 (3), 489–493.

Fei, L., Wang, Y., 2022a. An optimization model for rescuer assignments under an uncertain environment by using Dempster-Shafer theory. Knowl.-Based Syst. 109680.

Fei, L., Wang, Y., 2022b. Demand prediction of emergency materials using case-based reasoning extended by the Dempster-Shafer theory. Socio-Econ. Plan. Sci. 101386.

Fu, C., Ding, X., Chang, W., 2022. An interval-valued linguistic Markov decision model with fast convergency. Eng. Appl. Artif. Intell. 114, 105158.

Fujita, H., Ko, Y.-C., 2020. A heuristic representation learning based on evidential memberships: Case study of UCI-SPECTF. Internat. J. Approx. Reason. 120, 125–137.

Guo, X., Xin, X., 2005. Partial entropy and relative entropy of fuzzy sets. Fuzzy Syst. Math. 19 (2), 97–102.

Huang, J., Fan, Y., Xiao, F., 2023. On some bridges to complex evidence theory. Eng. Appl. Artif. Intell. 117, 105605.

Lai, J.W., Cheong, K.H., 2020. Superposition of COVID-19 waves, anticipating a sustained wave, and lessons for the future. BioEssays 42 (12), 2000178.

Lai, H., Liao, H., 2021. A multi-criteria decision making method based on DNMA and CRITIC with linguistic D numbers for blockchain platform evaluation. Eng. Appl. Artif. Intell. 101, 104200.

Li, D., Deng, Y., Cheong, K.H., 2021. Multisource basic probability assignment fusion based on information quality. Int. J. Intell. Syst. 36 (4), 1851–1875.

Li, Y., Pelusi, D., Cheong, K.H., Deng, Y., 2022. The arithmetics of two dimensional belief functions. Appl. Intell. 52 (4), 4192–4210.

Liu, R., Fei, L., Mi, J., 2022. An evidential MULTIMOORA approach to assessing disaster risk reduction education strategies under a heterogeneous linguistic environment. Int. J. Disaster Risk Reduct. 78, 103114.

Liu, Z., Liu, Y., Dezert, J., Cuzzolin, F., 2020a. Evidence combination based on credal belief redistribution for pattern classification. IEEE Trans. Fuzzy Syst. 28 (4), 618–631.

Liu, P., Zhang, X., Pedrycz, W., 2020b. A consensus model for hesitant fuzzy linguistic group decision-making in the framework of Dempster–Shafer evidence theory. Knowl.-Based Syst. 212, 106559.

Mao, S., Han, Y., Deng, Y., Pelusi, D., 2020. A hybrid DEMATEL-FRACTAL method of handling dependent evidences. Eng. Appl. Artif. Intell. 91, 103543.

Meng, D., Wang, H., Yang, S., Lv, Z., Hu, Z., Wang, Z., 2022. Fault analysis of wind power rolling bearing based on EMD feature extraction. CMES-Comput. Model. Eng. Sci. 130 (1), 543–558.

Miao, W., Geng, J., Jiang, W., 2023. Multi-granularity decoupling network with pseudo-label selection for remote sensing image scene classification. IEEE Trans. Geosci. Remote Sens. http://dx.doi.org/10.1109/TGRS.2023.3244565.

Murphy, C.K., 2000. Combining belief functions when evidence conflicts. Decis. Support Syst. 29 (1), 1–9.

Ni, L., Chen, Y.-w., de Brujin, O., 2021. Towards understanding socially influenced vaccination decision making: An integrated model of multiple criteria belief modelling and social network analysis. European J. Oper. Res. 293 (1), 276–289.

Qiang, C., Deng, Y., Cheong, K.H., 2022. Information fractal dimension of mass function. Fractals 30, 2250110.

Shafer, G., 1976. A Mathematical Theory of Evidence, Vol. 42. Princeton University Press, pp. 237–238.

Shang, Q., Li, H., Deng, Y., Cheong, K.H., 2022. Compound credibility for conflicting evidence combination: An autoencoder-k-means approach. IEEE Trans. Syst. Man Cybern.: Syst. 52 (9), 5602–5610.

Song, Y., Deng, Y., 2021. Entropic explanation of power set. Int. J. Comput. Commun. Control 16 (4), 4413.

Tang, S.-W., Zhou, Z.-J., Hu, C.-H., Yang, J.-B., Cao, Y., 2021. Perturbation analysis of evidential reasoning rule. IEEE Trans. Syst. Man Cybern.: Syst. 51 (8), 4895–4910.

Tao, R., Liu, Z., Cai, R., Cheong, K.H., 2021. A dynamic group MCDM model with intuitionistic fuzzy set: Perspective of alternative queuing method. Inform. Sci. 555, 85–103.

Wang, Z., Hou, D., Gao, C., Huang, J., Xuan, Q., 2022a. A rapid source localization method in the early stage of large-scale network propagation. In: Proceedings of the ACM Web Conference (WWW-22). p. 1372.

Wang, Z., Mu, C., Hu, S., Chu, C., Li, X., 2022b. Modelling the dynamics of regret minimization in large agent populations: a master equation approach. In: Proceedings of the 31st International Joint Conference on Artificial Intelligence (IJCAI-22). pp. 534–540.

Wang, Z., Song, Z., Shen, C., Hu, S., 2023. Emergence of punishment in social dilemma with environmental feedback anonymous submission. In: Proceedings of the 37th AAAI Conference on Artificial Intelligence (AAAI-23). Accepted.

Wei, B., Xiao, F., Fang, F., Shi, Y., 2021. Velocity-free event-triggered control for multiple Euler—Lagrange systems with communication time delays. IEEE Trans. Automat. Control 66 (11), 5599–5605.

Wu, Q., Deng, Y., Xiong, N., 2022. Exponential negation of a probability distribution. Soft Comput. 26 (3), 2147–2156.

Xiao, F., 2019. Multi-sensor data fusion based on the belief divergence measure of evidences and the belief entropy. Inf. Fusion 46, 23–32.

Xiao, F., 2020. A new divergence measure for belief functions in D-S evidence theory for multisensor data fusion. Inform. Sci. 514, 462–483.

Xiao, F., 2022a. GEJS: A generalized evidential divergence measure for multisource information fusion. IEEE Trans. Syst. Man Cybern. - Syst. http://dx.doi.org/10.1109/TSMC.2022.3211498.

Xiao, F., 2022b. Generalized quantum evidence theory. Appl. Intell. http://dx.doi.org/10.1007/s10489--022--04181--0.

Xiao, F., Cao, Z., Lin, C.-T., 2022a. A complex weighted discounting multisource information fusion with its application in pattern classification. IEEE Trans. Knowl. Data Eng. http://dx.doi.org/10.1109/TKDE.2022.3206871.

Xiao, F., Pedrycz, W., 2022. Negation of the quantum mass function for multisource quantum information fusion with its application to pattern classification. IEEE Trans. Pattern Anal. Mach. Intell. 45 (2), 2054–2070.

Xiao, F., Wen, J., Pedrycz, W., 2022b. Generalized divergence-based decision making method with an application to pattern classification. IEEE Trans. Knowl. Data Eng. http://dx.doi.org/10.1109/TKDE.2022.3177896.

Xiong, L., Su, X., Qian, H., 2021. Conflicting evidence combination from the perspective of networks. Inform. Sci. 580, 408–418.

Xu, X., Zhang, D., Bai, Y., Chang, L., Li, J., 2020. Evidence reasoning rule-based classifier with uncertainty quantification. Inform. Sci. 516, 192–204.

Yager, R.R., 2021. Inferring the value of a variable using measure based information of a related variable. Eng. Appl. Artif. Intell. 101, 104201.

Yager, R.R., Alajlan, N., Bazi, Y., 2019. Uncertain database retrieval with measure-based belief function attribute values. Inform. Sci. 501, 761–770.

Zhang, S., Xiao, F., 2022. A TFN-based uncertainty modeling method in complex evidence theory for decision making. Inform. Sci. http://dx.doi.org/10.1016/j.ins.2022.11.014.

Zhou, Q., Deng, Y., 2022. Fractal-based belief entropy. Inform. Sci. 587, 265–282.

Zhou, M., Zheng, Y.-Q., Chen, Y.-W., Cheng, B.-Y., Herrera-Viedma, E., Wu, J., 2023. A large-scale group consensus reaching approach considering self-confidence with two-tuple linguistic trust/distrust relationship and its application in life cycle sustainability assessment. Inf. Fusion 94, 181–199.

Zhou, Y.-J., Zhou, M., Liu, X.-B., Cheng, B.-Y., Herrera-Viedma, E., 2022. Consensus reaching mechanism with parallel dynamic feedback strategy for large-scale group decision making under social network analysis. Comput. Ind. Eng. 174, 108818.

Zhu, C., Xiao, F., Cao, Z., 2022. A generalized Rényi divergence for multi-source information fusion with its application in EEG data analysis. Inform. Sci. 605, 225–243.